



King's Research Portal

DOI:

[10.1016/j.brainres.2017.07.002](https://doi.org/10.1016/j.brainres.2017.07.002)

Document Version

Peer reviewed version

[Link to publication record in King's Research Portal](#)

Citation for published version (APA):

Michielse, S., Gronenschild, E., Domen, P., van Os, J., & Marcelis, M. (2017). The details of structural disconnectivity in psychotic disorder: A family-based study of non-FA diffusion weighted imaging measures. *Brain research*. <https://doi.org/10.1016/j.brainres.2017.07.002>

Citing this paper

Please note that where the full-text provided on King's Research Portal is the Author Accepted Manuscript or Post-Print version this may differ from the final Published version. If citing, it is advised that you check and use the publisher's definitive version for pagination, volume/issue, and date of publication details. And where the final published version is provided on the Research Portal, if citing you are again advised to check the publisher's website for any subsequent corrections.

General rights

Copyright and moral rights for the publications made accessible in the Research Portal are retained by the authors and/or other copyright owners and it is a condition of accessing publications that users recognize and abide by the legal requirements associated with these rights.

- Users may download and print one copy of any publication from the Research Portal for the purpose of private study or research.
- You may not further distribute the material or use it for any profit-making activity or commercial gain
- You may freely distribute the URL identifying the publication in the Research Portal

Take down policy

If you believe that this document breaches copyright please contact librarypure@kcl.ac.uk providing details, and we will remove access to the work immediately and investigate your claim.

Accepted Manuscript

Research report

The details of structural disconnectivity in psychotic disorder: A family-based study of non-FA diffusion weighted imaging measures

Stijn Michielse, Ed Gronenschild, Patrick Domen, Jim van Os, Machteld Marcelis, for Genetic Risk, Outcome of Psychosis (G.R.O.U.P.),

PII: S0006-8993(17)30292-5

DOI: <http://dx.doi.org/10.1016/j.brainres.2017.07.002>

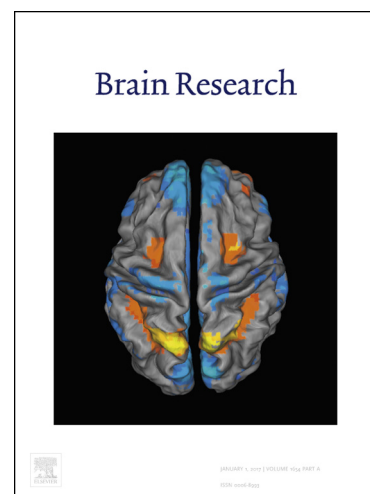
Reference: BRES 45416

To appear in: *Brain Research*

Received Date: 10 January 2017

Revised Date: 1 May 2017

Accepted Date: 4 July 2017



Please cite this article as: S. Michielse, E. Gronenschild, P. Domen, J. van Os, M. Marcelis, for Genetic Risk, Outcome of Psychosis (G.R.O.U.P.), The details of structural disconnectivity in psychotic disorder: A family-based study of non-FA diffusion weighted imaging measures, *Brain Research* (2017), doi: <http://dx.doi.org/10.1016/j.brainres.2017.07.002>

This is a PDF file of an unedited manuscript that has been accepted for publication. As a service to our customers we are providing this early version of the manuscript. The manuscript will undergo copyediting, typesetting, and review of the resulting proof before it is published in its final form. Please note that during the production process errors may be discovered which could affect the content, and all legal disclaimers that apply to the journal pertain.

The details of structural disconnectivity in psychotic disorder:

A family-based study of non-FA diffusion weighted imaging measures.

Stijn Michielse¹ MSc, Ed Gronenschild¹ PhD, Patrick Domen¹ MD, Jim van Os^{1,2} MD PhD, Machteld Marcelis^{1,3} MD PhD; for Genetic Risk and Outcome of Psychosis (G.R.O.U.P.)

¹ *Department of Psychiatry & Neuropsychology, School for Mental Health and Neuroscience, EURON, Maastricht University Medical Centre, PO Box 616, 6200 MD Maastricht, the Netherlands.*

² *King's College London, King's Health Partners, Department of Psychosis Studies, Institute of Psychiatry, London, UK.*

³ *Institute for Mental Health Care Eindhoven (GGzE), Eindhoven, the Netherlands.*

Address of correspondence:

Stijn Michielse

Dept. of Psychiatry & Neuropsychology, Maastricht University Medical Centre

PO Box 616, 6200 MD Maastricht, the Netherlands.

Tel: +31 43 3883881

Fax: +31 43 3884122

Email: stijn.michielse@maastrichtuniversity.nl

Abstract

Background: Diffusion Tensor Imaging (DTI) studies in psychotic disorder have shown reduced FA, often interpreted as disturbed white matter integrity. The observed ‘dysintegrity’ may be of multifactorial origin, as changes in FA are thought to reflect a combination of changes in myelination, fiber organization and number of axons. Examining the structural substrate of the diffusion tensor in individuals with (risk for) psychotic disorder may provide better understanding of the underlying structural changes.

Methods: DTI scans were acquired from 85 patients with psychotic disorder, 93 siblings of patients with psychotic disorder and 80 controls. Cross-sectional group comparisons were performed using Tract-Based Spatial Statistics (TBSS) on six DTI measures: axial diffusivity (AXD), radial diffusivity (RD), mean diffusivity (MD), and the case linear (CL), case planar (CP) and case spherical (CS) tensor shape measures.

Results: AXD did not differ between the groups. RD and CS values were significantly increased in patients compared to controls and siblings, with no significant differences between the latter two groups. MD was higher in patients compared to controls (but not siblings), with no difference between siblings and controls. CL was smaller in patients than in siblings and controls, and CP was smaller in both patients and siblings as compared to controls.

Conclusion: The differences between individuals with psychotic disorder and healthy controls, derived from detailed diffusion data analyses, suggest less fiber orientation and increased free water movement in the patients. There was some evidence for association with familial risk expressed by decreased fiber orientation.

Keywords:

Schizophrenia, white matter, nerve fibers, axons, anisotropy, siblings

1. Introduction

White matter integrity changes in psychotic disorder can be examined by measuring fractional anisotropy (FA). However, the FA provides information on white matter integrity combining myelination, fiber organization and number of axons in a single measure, making it a rather non-specific measure (Mori et al., 2006; O'Donnell et al., 2015). A systematic review on voxel-wise diffusion-weighted imaging (DWI) studies in psychotic disorder reported reduction of FA in the left frontal lobe and the temporal lobe (Ellison-Wright et al., 2009). In addition, lower FA in the splenium of the corpus callosum and the cingulum bundle may also be associated with psychotic disorder (Domen et al., 2013; Fitzsimmons et al., 2014). A more recent study found decreased FA in the right temporal lobe in a group with schizotypal personality disorder (Y. Sun et al., 2016). Furthermore, a review on early onset schizophrenia showed a widespread lower FA in patients relative to controls (Tamnes et al., 2016). The available evidence for individuals at higher than average genetic risk suggest that white matter integrity is reduced, compared with healthy controls, in the corpus callosum (Knochel et al., 2012), the inferior longitudinal fasciculus, the left inferior fronto-occipital fasciculus (Oestreich et al., 2015) and the superior longitudinal fasciculus (K. A. Clark et al., 2011; Nakamura et al., 2012; H. Sun et al., 2015), although not all studies agree (Domen et al., 2013).

As described above, FA alterations may have several origins. Therefore, additional DWI measures that provide more specific information on white matter integrity in psychotic disorder may be of interest. The axial diffusivity (AXD) describes the diffusion of water diffusion parallel to the white matter tracts (λ_1 , see Fig. 1) and may reflect axonal function related to the number of axons. A decrease in AXD may be indicative of axonal injury/loss (Song et al., 2003). The radial diffusivity (RD) measures the diffusion of water perpendicular to the white matter tracts and may be a marker for myelin content; an increase in RD indicates demyelination (Giorgio et al., 2008;

Song et al., 2005). Previous literature suggests that the disruption of connectivity in psychotic disorder may be associated with dysfunction in myelin maintenance and repair and less with a decrease in the number of axons (Davis et al., 2003; Ruef et al., 2012). Indeed, higher RD in the bilateral cortico-spinal tracts, left arcuate fasciculus (de Weijer et al., 2013) and right superior longitudinal fasciculus (Ruef et al., 2012) have been reported.

Mean diffusivity (MD) measures the total water diffusion; increased MD may indicate an increase in the cellular or interstitial fluid compartments (Narr et al., 2009). Psychotic disorder has consistently been associated with increased ventricular enlargement and an overall increase in cerebrospinal fluid (Shenton et al., 2001). This cerebrospinal fluid increase may originate from specific white matter alterations, such as demyelination. For example, previous studies on psychotic disorder have found an increase in free water movement (increased RD and MD) for commissural fibers and projection fibers (Scheel et al., 2013).

AXD and RD are related to respectively diffusion parallel and perpendicular to the of fiber tracts, while geometrical measures (tensor shapes) take all three eigenvalues into account (Fig. 1). With the tensor shape representation method, more knowledge on white matter composition, can be provided by specifying the linear (CL), spherical (CS), and planar (CP) tensor shape measures (Westin et al., 2002). An increase in CL may be related to increased anisotropy, which is associated with fibers being more oriented in one primary direction. In highly organized and myelinated white matter regions, such as the corpus callosum, CL will be high (Alexander et al., 2000; Westin et al., 2002).

CS is related to the diffusion of water in any direction, having no profound preferable direction. In highly isotropic matter, such as cerebrospinal fluid, the CS will be high because water molecules can go in any direction not having one distinct preference. The more isotropic, the

more spherical (CS towards one) the tensor becomes. CP is probably associated with fiber orientation and structure (Alexander et al., 2000). High CP reflects areas with increased complexity of the fiber orientation (Westin et al., 2002). The more crossing, kissing and twisting of the fibers in a plane, the more complex the fiber structure becomes and the higher the CP. High CP can, for example, be found in the arcuate fasciculus, because of the crossing and twisting of fibers and overlap of gray matter (Alexander et al., 2000).

Previously, we examined FA in the same sample as described in the present study, and found dispersed FA was reduced in the patient group (Domen et al, 2013). We now examined structural disconnectivity at a more fine-grained level, using the above-described six DWI measures. It was hypothesized that individuals with (risk of) psychotic disorder have altered DWI shape measures and that these are caused by alterations in fiber complexity and increased isotropic diffusion.

2. Results

2.1 Demographics and clinical data

Table 1 shows the demographic characteristics. Patients had a lower educational level compared to controls and siblings, and the proportion of males in the patient group was different from the control group. The frequency of lifetime cannabis and other drug use was higher in patients than in controls and siblings (Table 1).

Most of the patients were receiving antipsychotic medication (second generation: $n = 67$; first generation: $n = 3$). The mean current dosage of antipsychotic medication in terms of standard haloperidol equivalents was 5.5 milligrams (mg) (SD = 4.6). A total of 16 patients used antidepressants, 6 used benzodiazepines, 5 used anticonvulsants, and 2 used lithium. Three siblings and 3 control participants used antidepressants, and one control participant used benzodiazepines.

2.2 Whole brain differences in DWI measures

The reported skeleton mean values were calculated in R and the reported number of voxels were derived from *randomise* ($P < 0.05$ and $P < 0.01$; see Supplemental information) and this is true for all measures presented below.

2.2.1 Axial diffusivity

The mean AXD value did not show significant differences between the groups in any of the six comparisons.

2.2.2 Radial diffusivity

The mean RD value was significantly higher in patients ($0.00052 \text{ mm}^2/\text{s}$) compared to controls ($0.00050 \text{ mm}^2/\text{s}$) in 12838 voxels dispersed over the brain (Figure 2A). The following brain areas were significant using a more conservative threshold $P < 0.01$: right anterior limb internal capsule,

bilateral retrolenticular part of internal capsule, bilateral anterior/superior/posterior corona radiata, bilateral posterior corona radiata, bilateral sagittal striatum, bilateral external capsule, right superior longitudinal fasciculus, right superior fronto-occipital fasciculus, right uncinate fasciculus, bilateral tapetum and corpus callosum fibers (total number of voxels: 12048). In addition, the mean RD value was significantly higher in patients compared to siblings (0.00050 mm²/s) in a total of 13275 voxels dispersed over the brain (Figure 2B). The brain areas that survived the threshold of $P < 0.01$ were: bilateral anterior/superior/posterior corona radiata and corpus callosum fibers (total number of voxels: 8886). The RD value of siblings was not significantly different from controls.

2.2.3 Mean diffusivity

The mean MD value was higher in patients (0.00079 mm²/s) compared to controls (0.00078 mm²/s) in 7503 significant voxels (Figure 2C). Most voxels with higher MD values were found in bilateral projection and commissural fibers. The brain areas that survived the threshold of $P < 0.01$ were: bilateral retrolenticular part of internal capsule, bilateral anterior/superior corona radiata and corpus callosum fibers (total number of voxels: 5552). Patients had a slightly higher mean MD than siblings (0.00079 mm²/s), but not at the a priori set significance threshold. The mean MD value of siblings was not significantly different from controls.

2.2.4 Linear shape measure

The CL measure showed a lower value in patients (0.5273) compared to controls (0.5370) in 4715 significant voxels. Atlas labeling showed that all fiber types had decreased values, with a larger number of voxels in the right hemisphere (3037 voxels) than in the left hemisphere (1678 voxels) for patients compared to controls (Figure 3A). The left superior corona radiata, and the body of the corpus callosum (total number of voxels: 1929) were upheld using the threshold of $P < 0.01$. The patients had a lower CL compared to siblings (0.5348) in 10460 significant voxels,

with a slightly higher number of voxels in the right hemisphere for the projection and association fibers (Table 2 and Figure 3B). Using a more conservative threshold $P < 0.01$ the following regions were upheld: right anterior limb of internal capsule, bilateral anterior/superior corona radiata, right posterior corona radiata, right external capsule, right superior longitudinal fasciculus, right superior fronto-occipital fasciculus and the corpus callosum fibers (total number of voxels: 7748). The CL was lower in siblings compared to controls, but there was no significant difference.

2.2.5 Planar shape measure

The case planar (CP) showed a lower value in patients (0.1550) compared to controls (0.1567) in 6498 significant voxels. The decreased CP in patients over controls was more profound in the left hemisphere (4089 voxels) than in the right hemisphere (2409 voxels), and located in the projection and commissural fibers (Table 2). The following brain areas were significant using a more conservative threshold $P < 0.01$: left anterior/posterior limb of internal capsule, right retrolenticular part of internal capsule, bilateral anterior/superior/posterior corona radiata, left superior fronto-occipital fasciculus and the corpus callosum fibers (total number of voxels: 6462). Similarly, CP values were lower in siblings (0.1554) than in controls (0.1567) in 4200 significant voxels, with more voxels in the left (2819 voxels) than in the right (1381 voxels) hemisphere, and located in the projection and commissural fibers (Table 2). The bilateral anterior corona radiata, left superior corona radiata and genu/body of the corpus callosum (total number of voxels: 3431) survived the more conservative thresholding.

2.2.6 Spherical shape measure

The CS measure was higher in patients (0.3177) compared to controls (0.3063) in 17611 significant voxels (Figure 3C). The following brain areas were significant using a more conservative threshold $P < 0.01$: bilateral anterior/posterior limb internal capsule, bilateral

retrolenticular part of internal capsule, bilateral anterior/superior/posterior corona radiata, bilateral posterior corona radiata, right sagittal striatum, bilateral external capsule, left cingulum, bilateral fornix, bilateral superior longitudinal fasciculus, bilateral superior fronto-occipital fasciculus, right uncinate fasciculus, bilateral tapetum and corpus callosum fibers (total number of voxels: 17253). In addition, the CS was higher in patients compared to siblings (0.3099) in 13909 significant voxels (Figure 3D). The findings in the left retrolenticular part of internal capsule, bilateral anterior/superior/posterior corona radiata, bilateral posterior thalamic radiation, right superior longitudinal fasciculus, bilateral tapetum and the corpus callosum fibers (total number of voxels: 11190) were upheld at $P < 0.01$. Increased CS in patients and siblings was found in many white matter areas, with no significant difference between siblings and controls (Table 2). The areas with increased CS and decreased CL were partly overlapping.

2.3 Models with drug- and medication use

2.3.1 Cannabis and other drug use

Tract-based spatial statistics analyses did not show major differences in the amount of voxels detected in atlas labels when controlled for cannabis and other drug use (see supplementary Tables 1 - 4). Generally, the amount of significant voxels in all DWI measures increased slightly, and in some instances decreased slightly, when controlled for cannabis and other drugs.

2.3.2 Antipsychotic medication use

Controlling for medication use in tract-based spatial statistics showed an overall decrease of 4% in the amount of significant voxels detected in all group comparisons, with an exception for the CL measure where an increase in the patient-sibling comparison (projection fibers 2% for both left and right hemispheres) was found. Also the CS measure showed an increase in the amount of

voxels in the patient-sibling comparison (10% projection fibers and 19% association fibers right side) (data available on request).

There was no main effect of medication on the outcome measures. Antipsychotic medication use lifetime was non-significantly associated with any of the DWI measures in patients (AXD: $B = -7.49 \times 10^{-11}$, $P = 0.933$; RD: $B = -1.42 \times 10^{-10}$, $P = 0.815$; MD: $B = -1.21 \times 10^{-10}$, $P = 0.845$; CL: $B = -1.57 \times 10^{-7}$, $P = 0.679$; CP: $B = 8.25 \times 10^{-8}$, $P = 0.588$; CS: $B = 5.88 \times 10^{-8}$, $P = 0.884$).

3. Discussion

The results from this study in individuals with (increased risk for) psychotic disorder provide novel insights into microstructural connectivity and suggest less fiber orientation and increased free water movement in the patients. The study, showed an increase in RD in patients compared to controls and siblings, with no differences between the latter two groups. MD was increased in patients compared to controls, whereas AXD was not different between the groups. Furthermore, there was evidence for increased CS and decreased CL in patients compared to both controls and siblings. CP, in comparison with controls, showed a decrease in both patients and siblings.

3.1 Non-FA diffusivity measures

The absence of differences in AXD between patients and controls is consistent with previous whole brain voxel-wise studies (Kikinis et al., 2015; Lee et al., 2013; Reid et al., 2016; Scheel et al., 2013; Seal et al., 2008; Zeng et al., 2016), denoting preservation of axonal cells in the white matter (Song et al., 2003). This indicates that the decrease in FA in the patients, as reported previously (Domen et al., 2013), may not be related to a reduction in the number of axons. The results suggest that this also applies to individuals at higher than average genetic risk for schizophrenia. Only one previous study included siblings: this study reported decreased AXD, although in a much smaller sample ($n=33$) and based on a region of interest analysis of language fiber connections (Y. Sun et al., 2016).

The current study showed an increase in RD in patients compared to controls and siblings. Increased RD may reflect myelin loss rather than changes in the number of axons, as demonstrated in an animal study (Song et al., 2002). These demyelination processes (and less directed fibers) may also occur in human white matter (Beaulieu, 2002). In the present study, clusters of significantly increased RD were dispersed over the brain and also represented in the

corpus callosum of patients with psychotic disorder. Previous whole brain voxel-wise studies (K. Clark et al., 2012; Koch et al., 2011; Lu et al., 2011; Reid et al., 2016; Whitford et al., 2010) and region of interest based studies (McCarthy-Jones et al., 2015; Ohtani et al., 2014; Seitz et al., 2016) in psychotic disorder have found similar increases in RD, although some region of interest studies reported reduced RD in specific areas (Carletti et al., 2012; Kikinis et al., 2015; Koch et al., 2011). In addition, increased RD has been found in individuals at ultra high-risk for psychotic disorder (Carletti et al., 2012), suggesting that alterations may already be present in the prodromal stages. Similarly, RD changes in the left anterior thalamic radiation may be apparent in specific stages of psychotic disorder (Lagopoulos et al., 2013). In the current study, fewer areas with increased RD were present in the patient-sibling comparison than in the patient-control comparison. This might hint to less difference in RD between patients and siblings compared to patients and controls. MD was increased in patients compared to controls. An increase of free water molecules in the white matter may indicate an increase of isotropy and therefore an increase in MD. The MD can be seen as a marker for microstructural changes related to cerebrospinal fluid increase in psychotic disorder (Narr et al., 2009). However, MD captures the overall mean water molecular displacement in a volume (Brubaker et al., 2009), representing a non-specific measure and therefore unable to point to myelin or axonal alterations (O'Donnell et al., 2015). Increased MD in patients with psychotic disorder compared to healthy controls has been demonstrated in previous studies (Ardekani et al., 2011; K. A. Clark et al., 2011; Zeng et al., 2016) and concurs with the extensive literature on cerebrospinal fluid abnormalities in psychotic disorder (Narr et al., 2009). The MD increase in the present study was mainly localized in areas close to the lateral ventricles, which may be partly due to cerebrospinal fluid contamination (Metzler-Baddeley et al., 2012). From the current cross-sectional data-analyses, it is unclear whether cerebrospinal fluid alterations are cause or consequence of

demyelination processes in nearby white matter tracts, though there is some evidence for an influence of increased cerebrospinal fluid on white matter myelin composition (Narr et al., 2009). The MD in siblings did not differ significantly from MD in patients and controls, although siblings displayed intermediate MD values. In the sparse literature on MD to date there is no evidence of MD alterations in siblings as compared to healthy controls, and no evidence for an MD intermediate phenotype (K. A. Clark et al., 2011; Goghari et al., 2014). It cannot be ruled out that (part of the) MD alterations are caused by the complexity of the white matter microstructure (Vos et al., 2012). While the findings in AXD are in line with the literature some caution should be taken when interpreting the RD and MD findings.

3.2 Tensor shape measures

Besides the AXD and RD previously described, CL, CP, and CS may provide more specific information on alterations in psychotic disorder by measuring geometrical tensor properties (Wheeler-Kingshott et al., 2009). The tensor shape can be changed due to several factors and provides specific information on fiber orientation. Interestingly, CS was significantly increased in many white matter areas in patients compared to siblings and controls, with no significant difference between the latter, although with an intermediate position for the siblings. This may imply that the amount of cerebrospinal fluid is increased in these white matter areas, given that in cerebrospinal fluid the isotropy is maximized (Westin et al., 2002). However, whether microstructural white matter changes lead to increased cerebrospinal fluid or vice versa warrants further investigation.

In contrast to CS increase, CL was significantly decreased in patients compared to controls and siblings, again with an intermediate position for siblings. The decrease in CL may reflect less oriented fibers or alterations in the myelin sheets (Westin et al., 2002). Many white matter fibers

showed a generally decreased CL and increased CS in patients compared to controls (see Table 2).

CP is thought to be associated with fiber orientation. The finding of lower CP in both patients and siblings compared to controls may reflect less crossing and twisting fibers, making the white matter structure less oriented (Alexander et al., 2000). The left superior fronto-occipital fasciculus (interconnecting the occipital and frontal lobe) showed lower CP in patients compared to controls. These alterations may be related to auditory and/or visual hallucinations, as described by De Weijer and colleagues (de Weijer et al., 2013). In addition, fibers connecting the internal capsule showed lower CP mainly in the left hemisphere in patients and siblings.

Furthermore, a third area with lower CP in both patients and siblings, compared to controls, was the corpus callosum. However, findings in CP have to be interpreted with caution, since noise in the data may influence this measure more than the other tensor shape measures (Alexander et al., 2000).

In conclusion, these new findings on tensor shape measures in psychotic disorder may hint at alterations in fiber orientation rather than axonal loss. In addition, increased CS in combination with decreased CL and CP was found.

3.3 Cannabis use

Most fibers showed slight increases and some showed slight decreases in the amount of significant voxels when adding cannabis and other drug use to the tract-based spatial statistics models. In general, there was no evidence for major effects of these substances on any of the outcome measures. This fits with previous cross-sectional studies showing absence of associations between cannabis and white matter structure (DeLisi, 2008; Domen et al., 2013; Peters et al., 2010; Solowij et al., 2011). However, a study of patients with adolescent-onset

psychotic disorder with early cannabis use showed FA decrease in the internal capsule, corona radiata and superior and inferior longitudinal fasciculus with respect to controls (James et al., 2011). The study sample described by James and colleagues included relatively young participants compared to our sample and as white matter is still developing during adolescence, the impact of cannabis use may be more prominent in this stage of life. This is supported by a recent longitudinal, 18-months follow-up, study in adolescents with early onset psychotic disorder, showing that cannabis use during adolescence may lead to a decrease in FA in the left inferior longitudinal fasciculus and the left inferior fronto-occipital fasciculus (Epstein et al., 2015). As stated in recent reviews (Cookey et al., 2014; Lubman et al., 2015), more research is needed on the impact of cannabis use on risk for psychotic disorder.

3.4 Medication use

The results showed that there was a decrease in the amount of significant voxels for most of the outcome measures after correcting for cumulative antipsychotic medication exposure. However, there was no evidence for a main effect of antipsychotic medication on the six outcome measures. The exact influence of antipsychotic medication on FA alterations is not clear (Domen et al., 2013; Minami et al., 2003). However, a longitudinal study has described increased FA values after 12 weeks of clozapine exposure (Ozcelik-Eroglu et al., 2014). Another longitudinal study reported that AXD decreased (indicative of axonal loss) and RD increased (indicative of myelin preservation) over time, in response to antipsychotic medication use (Szeszko et al., 2014). Therefore, the influence of antipsychotic medication on myelin and axons within the white matter needs further attention and investigation.

3.5 Methodological considerations

A tract-based spatial statistics processing stream was used, in which only the white matter in the skeleton was taken into the analysis. This method reduces the amount of voxels and focuses only on the core of the main white matter tracts making it robust for group comparisons. Although this method is widely used, some detail on the white matter is lost and it may not be sensitive to detect changes in peripheral regions located on the skeleton (Edden et al., 2011). Moreover, the skeleton thickness and thus the statistical power depends on the orientation of the brain in the scanner (Edden et al., 2011). Finally, as with all voxel-based methods, registration of the FA data to a template may cause both type I and II errors (Jones et al., 2010).

Related to this consideration is the atlas labeling method. Most of the voxels, but not all, got a label and arbitrary borders are set in the specific atlases used. Therefore, some significant voxels located closely to borders were not assigned to the specific area delineated by the atlas.

Interpretation of the outcomes of the study is limited to the millimeter scale resolution, capturing many individual cells, while several processes like demyelination and axonal loss can take place within a single voxel (O'Donnell et al., 2011). With the protocol used it may not be possible to disambiguate the effects of microstructural architecture and pathological processes on our findings. More advanced scan acquisitions and analysis techniques are required to accomplish this complex task (Jones et al., 2013).

Since the application of tensor shape measures in psychotic disorder is relatively new, the results need replication. In addition, post-mortem research can add to the biological understanding of changes in diffusion tensor shape measures. Longitudinal assessment of shape measures may contribute to further interpretation and understanding of these measures in the neurobiology of psychotic disorder.

4. Conclusion

The study showed that geometrical tensor shape diffusion tensor measures might contribute to our understanding of the neurobiological alterations associated with psychotic disorder. Patients with psychotic disorder, and in part their siblings, showed changes at the level of white matter and may be related to alterations in fiber orientation rather than number of axons. The data support the notion that cerebral vulnerability underlying psychotic disorder may be detectable in white matter.

5. Methods and Materials

5.1 Participants

Data was collected in the context of a multicenter longitudinal study (Genetic Risk and Outcome of Psychosis, G.R.O.U.P) in the Netherlands. In selected representative geographical areas in the Netherlands and neighboring Belgium, patients were identified through representative clinicians providing health care for those with psychotic disorder. Siblings were contacted through participating patients. Mailings and advertisements were effectuated in local newspapers of the same geographical area in order to recruit control participants. The total sample consisted of 258 participants: 85 patients with a psychotic disorder, 93 siblings without a psychotic disorder and 80 healthy controls. Familial relatedness of the participants has been described previously (Domen et al., 2013). For the current analyses, baseline data were used.

Inclusion criteria were: age range 16-50 years, a good command of Dutch language and for patients: a diagnosis of non-affective psychotic disorder with an illness duration of <10 years. Siblings and controls did not have a lifetime diagnosis of any non-affective psychotic disorder. In addition, controls had no first-degree relative with a lifetime diagnosis of any psychotic disorder, assessed using the Family Interview for Genetic Studies (FIGS) (Maxwell, 1992). Diagnosis was based on the Diagnostic and Statistical Manual of Mental Disorder-IV (DSM-IV) criteria (APA, 2000), measured with the Comprehensive Assessment of Symptoms and History (CASH) interview (Andreasen et al., 1992). Patients were diagnosed as follows: schizophrenia (n=59), schizoaffective disorder (n=9), schizophreniform disorder (n=4), brief psychotic disorder (n=2), and psychotic disorder not otherwise specified (n=11). Psychopathology in the siblings and controls was also assessed and respectively 18 and 12 participants had a history of a major depressive disorder. None of these met the criteria for a current depressive episode.

All participants were screened before MRI scanning using the following exclusion criteria: brain injury with unconsciousness of > than 1 hour, meningitis or other neurological diseases with possible impact on brain structure or function, cardiac arrhythmia requiring medical treatment and severe claustrophobia. In addition, participants with metal corpora aliena were excluded from the study, as were women with intrauterine device status and (suspected) pregnancy. The standing ethics committee approved the study protocol, and all the participants gave written informed consent in accordance with the committee's guidelines.

5.2 Measures

Level of psychotic symptomatology at the time of scanning was assessed with the Positive and Negative Symptom Scale (PANSS) (Kay et al., 1987) in all three groups. The five factor model by van der Gaag and colleagues (van der Gaag et al., 2006) was used.

Level of education was defined as the highest accomplished level of education.

Handedness was assessed using the Annett Handedness Scale (Annett, 1970), ranging from +100 (fully right-handed) to -100 (fully left-handed).

In the patient group, antipsychotic (AP) medication use was determined by patient report and verified with the treating consultant psychiatrist. Best estimate lifetime (cumulative) antipsychotic medication use was determined by multiplying the number of days of antipsychotic medication use with the corresponding haloperidol equivalents and summing these scores for all periods of antipsychotic medication use (including the exposure period between baseline assessment for the G.R.O.U.P. study and the moment of baseline MRI scanning), using the standard conversion formulas for antipsychotic medication dose equivalents described by Andreasen and colleagues (Andreasen et al., 2010).

Substance use was measured with the Composite International Diagnostic Interview (CIDI) sections B-J-L (WHO, 1990). Use of cannabis and other drugs was assessed as reported frequency of use during the last 12 months, as well as lifetime use. CIDI frequency data on lifetime cannabis and other drug use was available for respectively 250 participants (3% missing data) and 256 participants (1% missing data).

Alcohol use was defined as the reported number of weekly consumptions during the last 12 months.

5.3 MRI data acquisition

Magnetic resonance imaging scans were obtained at Maastricht University, the Netherlands, using an Allegra syngo MR A30 (Siemens, Erlangen, Germany) operating at 3.0 Tesla. The following anatomical scan parameters were used: Modified Driven Equilibrium Fourier Transform (MDEFT) sequence; 176 slices, 1 mm isotropic voxel size, echo time 2.4 msec, repetition time 7.92 msec, inversion time 910 msec, flip angle 15°, total acquisition time 12 min 51 sec; Magnetization Prepared Rapid Acquisition Gradient-Echo (MPRAGE; Alzheimer's Disease Neuroimaging Initiative) sequence 192 slices, 1 mm isotropic voxel size, echo time 2.6 msec, repetition time 2250 msec, inversion time 900 msec, flip angle 9°, total acquisition time 7 min 23 sec. The matrix size was 256 x 256 and field of view was 256 x 256 mm². The number of excitations was one. Two sequences were used because of a scanner update during data collection.

Microstructural anatomy was examined using diffusion tensor imaging with an echo-planar-imaging sequence (field of view 230 x 230 mm², TR 10800 ms, TE 84 ms, voxel size 1.8 x 1.8 x 1.8 mm³, b-value 1000 s/mm², noise level 40, 85 slices, no overlap). As a result of the scanner update, two DTI sequences were used: one with 76 directions (of which 4 T2-weighted (B0) and

72 diffusion-weighted (B)), and one with 81 directions (8xB0 and 73xB). The proportion of scans with 76 directions was balanced between the groups (78% in controls, 75% in siblings and 69% in patients ($\chi^2=1.52$, $P=0.468$), preventing any systematic bias. Total acquisition time of the DTI sequence was 15 minutes.

5.4 Data preprocessing

Raw DICOM images were converted to NIfTI standard using the tool “dcm2nii” from the MRICron software package (Rorden et al., 2000) and T1 data were cropped to remove slices containing background noise. All imaging data were visually inspected for artifacts and only data without artifacts got included.

5.5 DWI processing

DWI data were processed in ExploreDTI v4.8.3 (Leemans, Jeurissen, et al., 2009) in a MatLab (The MathWorks, Inc., Natick, Massachusetts, United States) programming environment. Subject motion and eddy-current induced geometrical distortions were corrected by realigning the DW images to the B0 images incorporating B-matrix rotation (Leemans & Jones, 2009). The DWI data were coregistered to the individual's T1 data to correct for echo-planar imaging (EPI) distortion (Irfanoglu et al., 2012; Klein et al., 2010). Next, diffusion tensors were estimated using the Robust Estimation of Tensors by the Outlier Rejection (RESTORE) method (Chang et al., 2005). Finally, eigenvalue-maps per dataset were produced providing the primary (λ_1), secondary (λ_2) and tertiary (λ_3) eigenvalues sorted in decreasing order, all expressed in mm^2/s . The AXD is equal to the λ_1 , RD is the average of λ_2 and λ_3 and the mean diffusivity (MD) is the average of λ_1 , λ_2 and λ_3 . In addition, geometrical tensor shape measures CL $((\lambda_1 - \lambda_2) / \lambda_1)$, CS (λ_3

$/\lambda_1$) and CP $((\lambda_2 - \lambda_3) / \lambda_1)$ were calculated (Westin et al., 2002). All measures were calculated using an in-house build MatLab script.

Subsequent analysis of the six DWI measures was performed using tract-based spatial statistics v1.2 in FSL 4.1.6 (FMRIB Analysis Group, Oxford, UK, <http://www.fmrib.ox.ac.uk/analysis/research/tbss/TBSS>). Non-linear registration aligned each FA volume to 1 x 1 x 1 mm standard FMRIB58_FA space containing a template derived from high-resolution images of 58 participants in a well-aligned population (Smith et al., 2006). After co-registration, a group mean FA skeleton was derived and thresholded at 0.25 to obtain the major white matter pathways, to exclude smaller peripheral tracts that would cause excess inter-participant variability, and to diminish non-linear registration misalignments. In addition, this threshold setting avoided inclusion of regions that are likely to be composed of multiple tissue types or fiber orientations. Finally, each registered FA volume was projected onto this skeleton and concatenated into a 4D volume containing the FA skeletonised data to be used for voxel-wise group comparison. In a similar way, using the warps from the FA volumes and the thresholded FA skeleton, the AXD, RD, MD, CL, CP and CS 4D skeletonised data were derived for voxel-wise group comparisons.

5.6 Statistical analyses

Statistical voxel-wise group analysis on the AXD, RD, MD, CL, CP and CS skeletons was based on linear model permutation testing (Anderson et al., 2001) by means of “randomise” in FSL (v2.1) controlling the family-wise error (FWE) (Winkler et al., 2014). The threshold-free cluster enhancement (TFCE) option (Smith et al., 2009) was enabled to find clusters without setting an initial cluster level. Statistical maps, corrected for multiple comparisons, were used for assessing differences between groups. A total of six contrasts per DWI measure were created to test for

significant ($P < 0.05$) differences: i) patients have higher/lower outcome measures than controls, ii) siblings have higher/lower outcome measures than controls, and iii) patients have higher/lower outcome measures than siblings. The a priori hypothesized confounding variables age, sex, handedness and level of education and lifetime (non-) cannabis/other drug use were used in the statistical models. The models with and without drug use were compared. Additionally, cumulative antipsychotic medication exposure was added as an additional covariate to the model in tract-based spatial statistics.

A number of 10,000 permutations were applied to reduce the error margin to an acceptable level of 8.7%, corresponding to ± 0.0044 at $P = 0.05$. After the randomisation testing, the statistical maps were thresholded at a level of $P < 0.05$ (and $P < 0.01$ to correct for multiple testing) and assigned with a label from a specific white matter tract name. Labels were taken from the Johns Hopkins University International Consortium for Brain Mapping (JHU-ICBM)-DTI-81 white-matter atlas (Mori et al., 2008) and the JHU white-matter tractography atlas (Hua et al., 2008). Combining these two label atlases provided sufficient coverage of the significant voxels produced by *randomise*.

All fibers were grouped based on different types of fiber systems: projection, association and commissural fibers. This provided a total of 7 projection and 8 association fibers both left and right separately. The fornix (column and body of the fornix) and the 3 corpus callosum fiber types were taken as a whole, except for the tapetum (for which left and right were separated). Additionally, the forceps minor and major from the JHU white-matter tractography atlas were included as a whole.

To extend the tract-based spatial statistics analyses with multilevel random regression, taking into account the familial relatedness of the individuals, mean DWI value per area from all six diffusion measures were extracted from the tract-based spatial statistics skeleton and exported to R version 3.2.0 (Team, 2008). Associations between group and respectively AXD, RD, MD, CL, CP, and CS measures were examined using a hierarchical ‘long format’ dataset, with the 38 regions (level 1) nested in participants (level 2) being part of families (level 3), with the number of voxels per region used as an analytic weight factor and with region as covariate. The “lme” package was used to fit these multilevel random regression models, with the six different DWI measures as the dependent variables and participant/family number modeled as random effects with age, sex, handedness and level of education as covariates.

In patients, associations between the cumulative lifetime antipsychotic medication dose and the respective DWI measures were examined and expressed by regression coefficients (B).

Acknowledgements

We thank Truda Driesen and Inge Crolla for their coordinating roles in the data collection, as well as the G.R.O.U.P. investigators: Richard Bruggeman, Wiepke Cahn, Lieuwe de Haan, René S. Kahn, Carin Meijer, Inez Myin-Germeys, Jim van Os and Durk Wiersma.

Financial disclosures

J. van Os is or has been an unrestricted research grant holder with, or has received financial compensation as an independent symposium speaker from, Lilly, BMS, Lundbeck, Organon, Janssen, GlaxoSmithKline, AstraZeneca, Pfizer, and Servier. M. Marcelis has received financial compensation as an independent symposium speaker from Lilly and Janssen. P. Domen has received financial compensation as an independent symposium speaker from AstraZeneca. All other authors report no biomedical financial interests or potential conflicts of interest.

References

- Alexander, A. L., Hasan, K., Kindlmann, G., Parker, D. L., & Tsuruda, J. S. (2000). A geometric analysis of diffusion tensor measurements of the human brain. *Magnetic Resonance in Medicine*, 44(2), 283-291.
- Anderson, M. J., & Robinson, J. (2001). Permutation tests for linear models. *Australian & New Zealand Journal of Statistics*, 43(1), 75-88. doi:10.1111/1467-842x.00156
- Andreasen, N. C., Flaum, M., & Arndt, S. (1992). The Comprehensive Assessment of Symptoms and History (CASH). An instrument for assessing diagnosis and psychopathology. *Arch Gen Psychiatry*, 49(8), 615-623.
- Andreasen, N. C., Pressler, M., Nopoulos, P., Miller, D., & Ho, B. C. (2010). Antipsychotic dose equivalents and dose-years: a standardized method for comparing exposure to different drugs. *Biological Psychiatry*, 67(3), 255-262. doi:10.1016/j.biopsych.2009.08.040
- Annett, M. (1970). A classification of hand preference by association analysis. *British Journal of Psychology*, 61(3), 303-321.
- APA. (2000). Diagnostic and statistical manual of mental disorders, 4th ed. Washington, DC: American Psychiatric Association.
- Ardekani, B. A., Tabesh, A., Sevy, S., Robinson, D. G., Bilder, R. M., & Szeszko, P. R. (2011). Diffusion tensor imaging reliably differentiates patients with schizophrenia from healthy volunteers. *Hum Brain Mapp*, 32(1), 1-9.
- Beaulieu, C. (2002). The basis of anisotropic water diffusion in the nervous system - a technical review. *NMR Biomed*, 15(7-8), 435-455. doi:10.1002/nbm.782
- Brubaker, C. J., Schmithorst, V. J., Haynes, E. N., Dietrich, K. N., Egelhoff, J. C., Lindquist, D. M., . . . Cecil, K. M. (2009). Altered myelination and axonal integrity in adults with childhood lead exposure: a diffusion tensor imaging study. *Neurotoxicology*, 30(6), 867-875. doi:10.1016/j.neuro.2009.07.007
- Carletti, F., Woolley, J. B., Bhattacharyya, S., Perez-Iglesias, R., Fusar Poli, P., Valmaggia, L., . . . McGuire, P. K. (2012). Alterations in white matter evident before the onset of psychosis. *Schizophrenia Bulletin*, 38(6), 1170-1179.
- Chang, L. C., Jones, D. K., & Pierpaoli, C. (2005). RESTORE: robust estimation of tensors by outlier rejection. *Magnetic Resonance in Medicine*, 53(5), 1088-1095. doi:10.1002/mrm.20426
- Clark, K., Narr, K. L., O'Neill, J., Levitt, J., Siddarth, P., Phillips, O., . . . Caplan, R. (2012). White matter integrity, language, and childhood onset schizophrenia. *Schizophr Res*, 138(2-3), 150-156. doi:10.1016/j.schres.2012.02.016
- Clark, K. A., Nuechterlein, K. H., Asarnow, R. F., Hamilton, L. S., Phillips, O. R., Hageman, N. S., . . . Narr, K. L. (2011). Mean diffusivity and fractional anisotropy as indicators of disease and genetic liability to schizophrenia. *Journal of Psychiatric Research*, 45(7), 980-988. doi:10.1016/J.Jpsychires.2011.01.006
- Cookey, J., Bernier, D., & Tibbo, P. G. (2014). White matter changes in early phase schizophrenia and cannabis use: An update and systematic review of diffusion tensor imaging studies. *Schizophr Res*, 156(2-3), 137-142. doi:10.1016/j.schres.2014.04.026
- Davis, K. L., Stewart, D. G., Friedman, J. I., Buchsbaum, M., Harvey, P. D., Hof, P. R., . . . Haroutunian, V. (2003). White matter changes in schizophrenia: evidence for myelin-related dysfunction. *Arch Gen Psychiatry*, 60(5), 443-456. doi:10.1001/archpsyc.60.5.443
- de Weijer, A. D., Neggers, S. F., Diederens, K. M., Mandl, R. C., Kahn, R. S., Hulshoff Pol, H. E., & Sommer, I. E. (2013). Aberrations in the arcuate fasciculus are associated with

- auditory verbal hallucinations in psychotic and in non-psychotic individuals. *Hum Brain Mapp*, 34(3), 626-634. doi:10.1002/hbm.21463
- DeLisi, L. E. (2008). The effect of cannabis on the brain: can it cause brain anomalies that lead to increased risk for schizophrenia? *Curr Opin Psychiatry*, 21(2), 140-150. doi:10.1097/YCO.0b013e3282f51266
- Domen, P. A., Michielse, S., Gronenschild, E., Habets, P., Roebroek, A., Schruers, K., . . . for, G. R. O. U. P. (2013). Microstructural white matter alterations in psychotic disorder: A family-based diffusion tensor imaging study. *Schizophr Res*, 146(1-3), 291-300. doi:10.1016/j.schres.2013.03.002
- Edden, R. A., & Jones, D. K. (2011). Spatial and orientational heterogeneity in the statistical sensitivity of skeleton-based analyses of diffusion tensor MR imaging data. *J Neurosci Methods*, 201(1), 213-219. doi:10.1016/j.jneumeth.2011.07.025
- Ellison-Wright, I., & Bullmore, E. (2009). Meta-analysis of diffusion tensor imaging studies in schizophrenia. *Schizophr Res*, 108(1-3), 3-10. doi:10.1016/j.schres.2008.11.021
- Epstein, K. A., & Kumra, S. (2015). White matter fractional anisotropy over two time points in early onset schizophrenia and adolescent cannabis use disorder: A naturalistic diffusion tensor imaging study. *Psychiatry Research-Neuroimaging*, 232(1), 34-41. doi:10.1016/j.psychresns.2014.10.010
- Fitzsimmons, J., Schneiderman, J. S., Whitford, T. J., Swisher, T., Niznikiewicz, M. A., Pelavin, P. E., . . . Kubicki, M. (2014). Cingulum bundle diffusivity and delusions of reference in first episode and chronic schizophrenia. *Psychiatry Res*, 224(2), 124-132. doi:10.1016/j.psychresns.2014.08.002
- Giorgio, A., Watkins, K. E., Douaud, G., James, A. C., James, S., De Stefano, N., . . . Johansen-Berg, H. (2008). Changes in white matter microstructure during adolescence. *Neuroimage*, 39(1), 52-61. doi:10.1016/j.neuroimage.2007.07.043
- Goghari, V. M., Billiet, T., Sunaert, S., & Emsell, L. (2014). A diffusion tensor imaging family study of the fornix in schizophrenia. *Schizophr Res*, 159(2-3), 435-440. doi:10.1016/j.schres.2014.09.037
- Hua, K., Zhang, J., Wakana, S., Jiang, H., Li, X., Reich, D. S., . . . Mori, S. (2008). Tract probability maps in stereotaxic spaces: analyses of white matter anatomy and tract-specific quantification. *Neuroimage*, 39(1), 336-347. doi:10.1016/j.neuroimage.2007.07.053
- Irfanoglu, M. O., Walker, L., Sarlls, J., Marengo, S., & Pierpaoli, C. (2012). Effects of image distortions originating from susceptibility variations and concomitant fields on diffusion MRI tractography results. *Neuroimage*, 61(1), 275-288. doi:10.1016/j.neuroimage.2012.02.054
- James, A., Hough, M., James, S., Winmill, L., Burge, L., Nijhawan, S., . . . Zarei, M. (2011). Greater white and grey matter changes associated with early cannabis use in adolescent-onset schizophrenia (AOS). *Schizophr Res*, 128(1-3), 91-97.
- Jones, D. K., & Cercignani, M. (2010). Twenty-five pitfalls in the analysis of diffusion MRI data. *NMR Biomed*, 23(7), 803-820. doi:10.1002/nbm.1543
- Jones, D. K., Knosche, T. R., & Turner, R. (2013). White matter integrity, fiber count, and other fallacies: the do's and don'ts of diffusion MRI. *Neuroimage*, 73, 239-254. doi:10.1016/j.neuroimage.2012.06.081
- Kay, S. R., Fiszbein, A., & Opler, L. A. (1987). The positive and negative syndrome scale (PANSS) for schizophrenia. *Schizophrenia Bulletin*, 13(2), 261-276.

- Kikinis, Z., Fitzsimmons, J., Dunn, C., Vu, M. A., Makris, N., Bouix, S., . . . Kubicki, M. (2015). Anterior commissural white matter fiber abnormalities in first-episode psychosis: a tractography study. *Schizophr Res*, 162(1-3), 29-34. doi:10.1016/j.schres.2015.01.037
- Klein, S., Staring, M., Murphy, K., Viergever, M. A., & Pluim, J. P. (2010). elastix: a toolbox for intensity-based medical image registration. *IEEE Trans Med Imaging*, 29(1), 196-205. doi:10.1109/TMI.2009.2035616
- Knochel, C., Oertel-Knochel, V., Schonmeyer, R., Rotarska-Jagiela, A., van de Ven, V., Prvulovic, D., . . . Linden, D. E. J. (2012). Interhemispheric hypoconnectivity in schizophrenia: Fiber integrity and volume differences of the corpus callosum in patients and unaffected relatives. *Neuroimage*, 59(2), 926-934. doi:10.1016/J.Neuroimage.2011.07.088
- Koch, K., Wagner, G., Schachtzabel, C., Schultz, C., Gullmar, D., Reichenbach, J., . . . Schlosser, R. (2011). Neural activation and radial diffusivity in schizophrenia: Combined fMRI and diffusion tensor imaging study. *British Journal of Psychiatry*, 198(3), 223-229. doi:<http://dx.doi.org/10.1192/bjp.bp.110.081836>
- Lagopoulos, J., Hermens, D. F., Hatton, S. N., Battisti, R. A., Tobias-Webb, J., White, D., . . . Hickie, I. B. (2013). Microstructural white matter changes are correlated with the stage of psychiatric illness. *Transl Psychiatry*, 3, e248. doi:10.1038/tp.2013.25
- Lee, S. H., Kubicki, M., Asami, T., Seidman, L. J., Goldstein, J. M., Meshulam-Gately, R. I., . . . Shenton, M. E. (2013). Extensive white matter abnormalities in patients with first-episode schizophrenia: a Diffusion Tensor Imaging (DTI) study. *Schizophr Res*, 143(2-3), 231-238. doi:10.1016/j.schres.2012.11.029
- Leemans, A., Jeurissen, B., Sijbers, J., & Jones, D. K. (2009). *ExploreDTI: a graphical toolbox for processing, analyzing, and visualizing diffusion MR data*. Paper presented at the 17th Annual Meeting of Intl Soc Mag Reson Med, Hawaii, USA.
- Leemans, A., & Jones, D. K. (2009). The B-Matrix Must Be Rotated When Correcting for Subject Motion in DTI Data. *Magnetic Resonance in Medicine*, 61(6), 1336-1349. doi:10.1002/Mrm.21890
- Lu, L. H., Zhou, X. J., Keedy, S. K., Reilly, J. L., & Sweeney, J. A. (2011). White matter microstructure in untreated first episode bipolar disorder with psychosis: comparison with schizophrenia. *Bipolar Disord*, 13(7-8), 604-613. doi:10.1111/j.1399-5618.2011.00958.x
- Lubman, D. I., Cheetham, A., & Yucel, M. (2015). Cannabis and adolescent brain development. *Pharmacol Ther*, 148, 1-16. doi:10.1016/j.pharmthera.2014.11.009
- Maxwell, M. (1992). Family Interview for Genetic Studies (FIGS): Manual For FIGS. *Clinical Neurogenetics Branch, Intramural Research Program, National Institute of Mental Health, Bethesda, MD*.
- McCarthy-Jones, S., Oestreich, L. K., Australian Schizophrenia Research, B., & Whitford, T. J. (2015). Reduced integrity of the left arcuate fasciculus is specifically associated with auditory verbal hallucinations in schizophrenia. *Schizophr Res*, 162(1-3), 1-6. doi:10.1016/j.schres.2014.12.041
- Metzler-Baddeley, C., O'Sullivan, M. J., Bells, S., Pasternak, O., & Jones, D. K. (2012). How and how not to correct for CSF-contamination in diffusion MRI. *Neuroimage*, 59(2), 1394-1403.
- Minami, T., Nobuhara, K., Okugawa, G., Takase, K., Yoshida, T., Sawada, S., . . . Kinoshita, T. (2003). Diffusion tensor magnetic resonance imaging of disruption of regional white matter in schizophrenia. *Neuropsychobiology*, 47(3), 141-145. doi:70583

- Mori, S., Oishi, K., Jiang, H., Jiang, L., Li, X., Akhter, K., . . . Mazziotta, J. (2008). Stereotaxic white matter atlas based on diffusion tensor imaging in an ICBM template. *Neuroimage*, 40(2), 570-582. doi:10.1016/j.neuroimage.2007.12.035
- Mori, S., & Zhang, J. (2006). Principles of diffusion tensor imaging and its applications to basic neuroscience research. *Neuron*, 51(5), 527-539. doi:10.1016/j.neuron.2006.08.012
- Nakamura, K., Kawasaki, Y., Takahashi, T., Furuichi, A., Noguchi, K., Seto, H., & Suzuki, M. (2012). Reduced white matter fractional anisotropy and clinical symptoms in schizophrenia: a voxel-based diffusion tensor imaging study. *Psychiatry Res*, 202(3), 233-238. doi:10.1016/j.psychres.2011.09.006
- Narr, K. L., Hageman, N., Woods, R. P., Hamilton, L. S., Clark, K., Phillips, O., . . . Nuechterlein, K. H. (2009). Mean diffusivity: a biomarker for CSF-related disease and genetic liability effects in schizophrenia. *Psychiatry Res*, 171(1), 20-32. doi:10.1016/j.psychres.2008.03.008
- O'Donnell, L. J., & Pasternak, O. (2015). Does diffusion MRI tell us anything about the white matter? An overview of methods and pitfalls. *Schizophr Res*, 161(1), 133-141. doi:10.1016/j.schres.2014.09.007
- O'Donnell, L. J., & Westin, C. F. (2011). An introduction to diffusion tensor image analysis. *Neurosurg Clin N Am*, 22(2), 185-196, viii. doi:10.1016/j.nec.2010.12.004
- Oestreich, L. K., McCarthy-Jones, S., Australian Schizophrenia Research, B., & Whitford, T. J. (2015). Decreased integrity of the fronto-temporal fibers of the left inferior occipito-frontal fasciculus associated with auditory verbal hallucinations in schizophrenia. *Brain Imaging Behav*. doi:10.1007/s11682-015-9421-5
- Ohtani, T., Bouix, S., Hosokawa, T., Saito, Y., Eckbo, R., Ballinger, T., . . . Kubicki, M. (2014). Abnormalities in white matter connections between orbitofrontal cortex and anterior cingulate cortex and their associations with negative symptoms in schizophrenia: A DTI study. *Schizophr Res*, 157(1-3), 190-197. doi:10.1016/j.schres.2014.05.016
- Ozcelik-Eroglu, E., Ertugrul, A., Oguz, K. K., Has, A. C., Karahan, S., & Yazici, M. K. (2014). Effect of clozapine on white matter integrity in patients with schizophrenia: a diffusion tensor imaging study. *Psychiatry Res*, 223(3), 226-235. doi:10.1016/j.psychres.2014.06.001
- Peters, B. D., Blaas, J., & de Haan, L. (2010). Diffusion tensor imaging in the early phase of schizophrenia: what have we learned? *Journal of Psychiatric Research*, 44(15), 993-1004. doi:10.1016/j.jpsychires.2010.05.003
- Reid, M. A., White, D. M., Kraguljac, N. V., & Lahti, A. C. (2016). A combined diffusion tensor imaging and magnetic resonance spectroscopy study of patients with schizophrenia. *Schizophr Res*, 170(2-3), 341-350. doi:10.1016/j.schres.2015.12.003
- Rorden, C., & Brett, M. (2000). Stereotaxic display of brain lesions. *Behav Neurol*, 12(4), 191-200.
- Ruef, A., Curtis, L., Moy, G., Bessero, S., Badan Ba, M., Lazeyras, F., . . . Merlo, M. (2012). Magnetic resonance imaging correlates of first-episode psychosis in young adult male patients: combined analysis of grey and white matter. *J Psychiatry Neurosci*, 37(5), 305-312. doi:10.1503/jpn.110057
- Scheel, M., Prokscha, T., Bayerl, M., Gallinat, J., & Montag, C. (2013). Myelination deficits in schizophrenia: evidence from diffusion tensor imaging. *Brain Struct Funct*, 218(1), 151-156. doi:10.1007/s00429-012-0389-2
- Seal, M. L., Yucel, M., Fornito, A., Wood, S. J., Harrison, B. J., Walterfang, M., . . . Pantelis, C. (2008). Abnormal white matter microstructure in schizophrenia: a voxelwise analysis of

- axial and radial diffusivity. *Schizophr Res*, 101(1-3), 106-110.
doi:10.1016/j.schres.2007.12.489
- Seitz, J., Zuo, J. X., Lyall, A. E., Makris, N., Kikinis, Z., Bouix, S., . . . Kubicki, M. (2016). Tractography Analysis of 5 White Matter Bundles and Their Clinical and Cognitive Correlates in Early-Course Schizophrenia. *Schizophrenia Bulletin*.
doi:10.1093/schbul/sbv171
- Shenton, M. E., Dickey, C. C., Frumin, M., & McCarley, R. W. (2001). A review of MRI findings in schizophrenia. *Schizophr Res*, 49(1-2), 1-52.
- Smith, S. M., Jenkinson, M., Johansen-Berg, H., Rueckert, D., Nichols, T. E., Mackay, C. E., . . . Behrens, T. E. J. (2006). Tract-based spatial statistics: Voxelwise analysis of multi-subject diffusion data. *Neuroimage*, 31(4), 1487-1505. doi:Doi 10.1016/J.Neuroimage.2006.02.024
- Smith, S. M., & Nichols, T. E. (2009). Threshold-free cluster enhancement: addressing problems of smoothing, threshold dependence and localisation in cluster inference. *Neuroimage*, 44(1), 83-98. doi:10.1016/j.neuroimage.2008.03.061
- Solowij, N., Yucel, M., Respondek, C., Whittle, S., Lindsay, E., Pantelis, C., & Lubman, D. I. (2011). Cerebellar white-matter changes in cannabis users with and without schizophrenia. *Psychological Medicine*, 41(11), 2349-2359.
doi:10.1017/S003329171100050X
- Song, S. K., Sun, S. W., Ju, W. K., Lin, S. J., Cross, A. H., & Neufeld, A. H. (2003). Diffusion tensor imaging detects and differentiates axon and myelin degeneration in mouse optic nerve after retinal ischemia. *Neuroimage*, 20(3), 1714-1722.
- Song, S. K., Sun, S. W., Ramsbottom, M. J., Chang, C., Russell, J., & Cross, A. H. (2002). Demyelination revealed through MRI as increased radial (but unchanged axial) diffusion of water. *Neuroimage*, 17(3), 1429-1436. doi:Doi 10.1006/Nimg.2002.1267
- Song, S. K., Yoshino, J., Le, T. Q., Lin, S. J., Sun, S. W., Cross, A. H., & Armstrong, R. C. (2005). Demyelination increases radial diffusivity in corpus callosum of mouse brain. *Neuroimage*, 26(1), 132-140. doi:10.1016/j.neuroimage.2005.01.028
- Sun, H., Lui, S., Yao, L., Deng, W., Xiao, Y., Zhang, W., . . . Gong, Q. (2015). Two Patterns of White Matter Abnormalities in Medication-Naïve Patients With First-Episode Schizophrenia Revealed by Diffusion Tensor Imaging and Cluster Analysis. *JAMA Psychiatry*, 72(7), 678-686. doi:10.1001/jamapsychiatry.2015.0505
- Sun, Y., Zhang, L., Ancharaz, S. S., Cheng, S., Sun, W., Wang, H., & Sun, Y. (2016). Decreased fractional anisotropy values in two clusters of white matter in patients with schizotypal personality disorder: A DTI study. *Behav Brain Res*, 310, 68-75.
doi:10.1016/j.bbr.2016.05.022
- Szeszko, P. R., Robinson, D. G., Ikuta, T., Peters, B. D., Gallego, J. A., Kane, J., & Malhotra, A. K. (2014). White matter changes associated with antipsychotic treatment in first-episode psychosis. *Neuropsychopharmacology*, 39(6), 1324-1331. doi:10.1038/npp.2013.288
- Tamnes, C. K., & Agartz, I. (2016). White Matter Microstructure in Early-Onset Schizophrenia: A Systematic Review of Diffusion Tensor Imaging Studies. *Journal of the American Academy of Child and Adolescent Psychiatry*, 55(4), 269-279.
doi:10.1016/j.jaac.2016.01.004
- Team, R. D. C. (2008). R: A language and environment for statistical computing. Retrieved from <http://www.R-project.org>
- van der Gaag, M., Hoffman, T., Remijsen, M., Hijman, R., de Haan, L., van Meijel, B., . . . Wiersma, D. (2006). The five-factor model of the Positive and Negative Syndrome Scale

- II: a ten-fold cross-validation of a revised model. *Schizophr Res*, 85(1-3), 280-287.
doi:10.1016/j.schres.2006.03.021
- Vos, S. B., Jones, D. K., Jeurissen, B., Viergever, M. A., & Leemans, A. (2012). The influence of complex white matter architecture on the mean diffusivity in diffusion tensor MRI of the human brain. *Neuroimage*, 59(3), 2208-2216. doi:10.1016/j.neuroimage.2011.09.086
- Westin, C. F., Maier, S. E., Mamata, H., Nabavi, A., Jolesz, F. A., & Kikinis, R. (2002). Processing and visualization for diffusion tensor MRI. *Med Image Anal*, 6(2), 93-108.
- Wheeler-Kingshott, C. A. M., & Cercignani, M. (2009). About "Axial" and "Radial" Diffusivities. *Magnetic Resonance in Medicine*, 61(5), 1255-1260.
doi:10.1002/mrm.21965
- Whitford, T., Kubicki, M., Schneiderman, J., O'Donnell, L., King, R., Alvarado, J., . . . Shenton, M. (2010). Corpus Callosum Abnormalities and Their Association with Psychotic Symptoms in Patients with Schizophrenia. *Biol Psychiatry*, 68(1), 70-77.
doi:<http://dx.doi.org/10.1016/j.biopsych.2010.03.025>
- WHO. (1990). Composite International Diagnostic Interview (CIDI). (Geneva: World Health Organization).
- Winkler, A. M., Ridgway, G. R., Webster, M. A., Smith, S. M., & Nichols, T. E. (2014). Permutation inference for the general linear model. *Neuroimage*, 92, 381-397.
doi:10.1016/j.neuroimage.2014.01.060
- Zeng, B., Ardekani, B. A., Tang, Y., Zhang, T., Zhao, S., Cui, H., . . . Wang, J. (2016). Abnormal white matter microstructure in drug-naïve first episode schizophrenia patients before and after eight weeks of antipsychotic treatment. *Schizophr Res*, 172(1-3), 1-8.
doi:10.1016/j.schres.2016.01.051

Figure legend

- Figure 1. Diffusion tensor model depicted by three eigenvectors.
- Figure 2. Statistical significance maps for RD (A: patients > controls and B: patients > siblings) and MD (C: patients > controls) overlaid on the white matter skeleton (in green) and the standard MNI space ($Z=98$). The patient-sibling comparison for MD did not show any significant differences. Images are radiologically oriented (participant's left is to the right).
- Figure 3. Statistical significance maps for CL (A: patients < controls and B: patients < siblings) and CS (C: patients > controls and D: patients > siblings) overlaid on the white matter skeleton (in green) and the standard MNI space ($Z=95$). Images are radiologically oriented (participant's left is to the right).

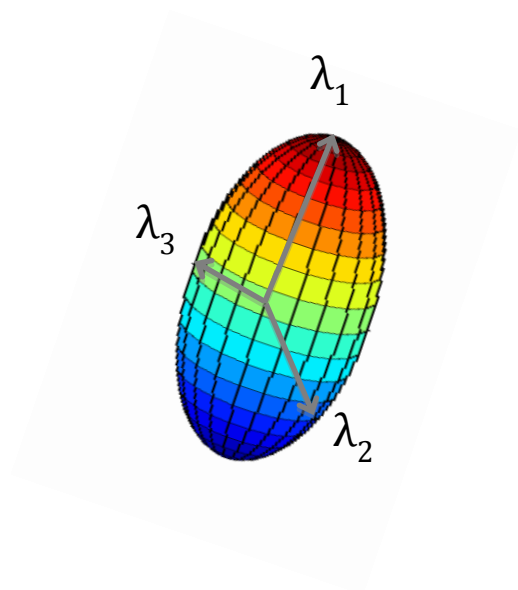
Figures

Figure 1. Diffusion tensor model depicted by three eigenvectors.

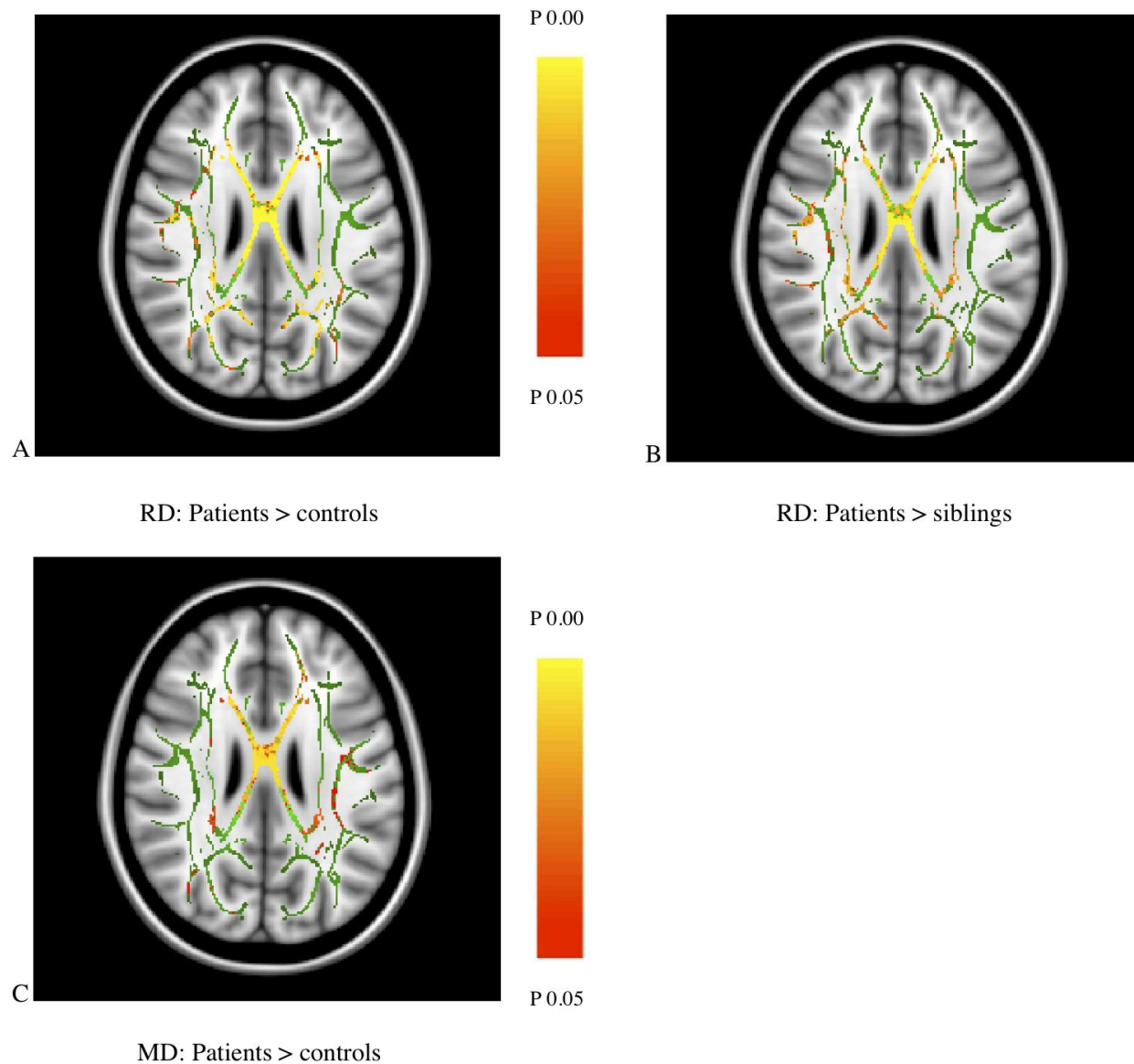


Figure 2. Statistical significance maps for RD (A: patients > controls and B: patients > siblings) and MD (C: patients > controls) overlaid on the white matter skeleton (in green) and the standard MNI space (Z=98). The patient-sibling comparison for MD did not show any significant differences. Images are radiologically oriented (participant's left is to the right).

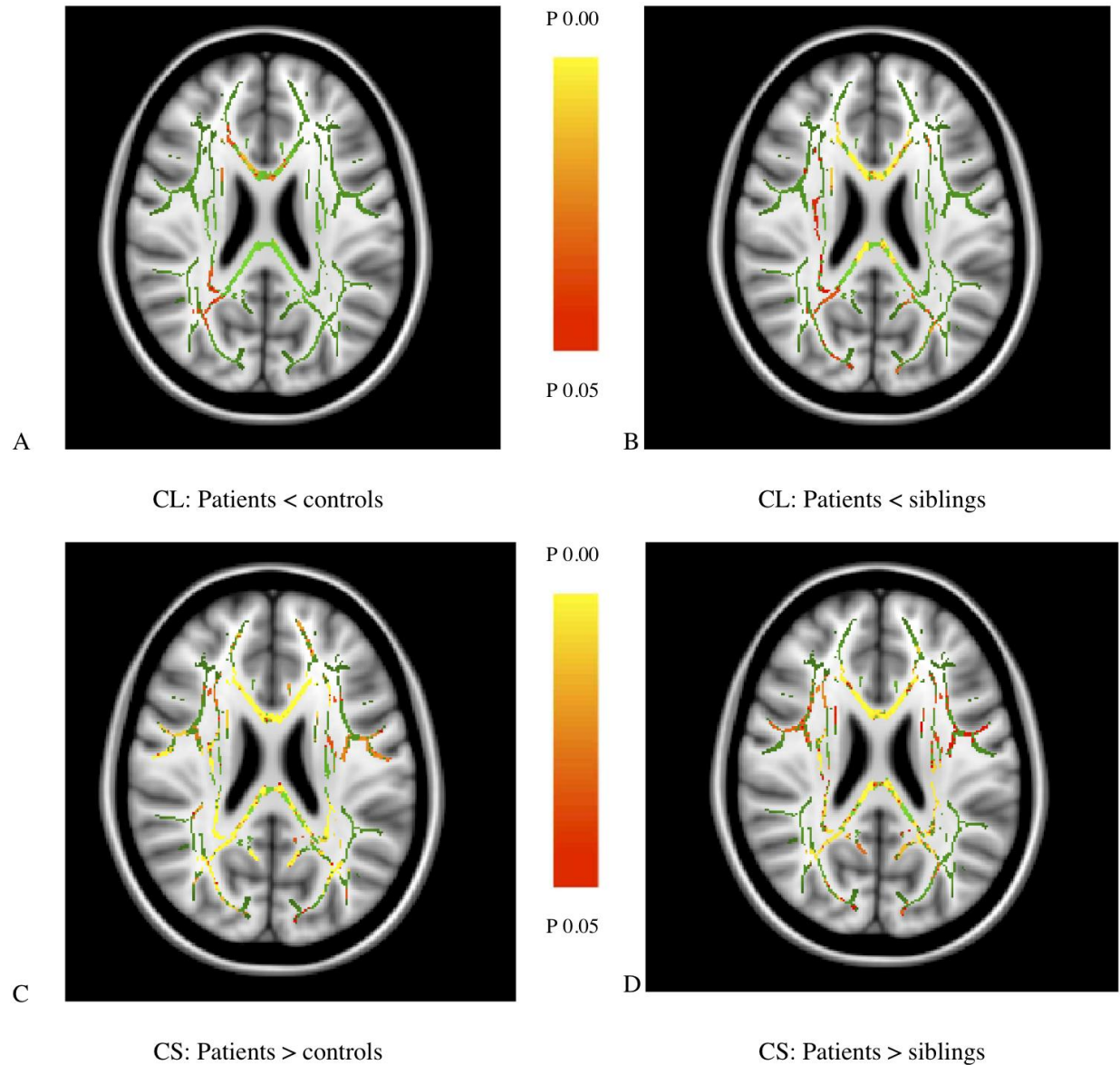


Figure 3. Statistical significance maps for CL (A: patients < controls and B: patients < siblings) and CS (C: patients > controls and D: patients > siblings) overlaid on the white matter skeleton (in green) and the standard MNI space (Z=95). Images are radiologically oriented (participant's left is to the right).

Tables

Table 1. Demographical characteristics.

	Controls (n=80)	Siblings (n=93)	Patients (n=85)
Age (years)	30.8±10.8	29.4±8.8	28.3±7.0
Handedness	76.3	73.9	72.9
Education (level)	5.4±1.8	5.1±2.1	4.1±2.0
Male sex (%)	29 (36%)	49 (53%)	58 (68%)
Age of onset (years)	-	-	22.8±6.4
Illness duration (years)	-	-	5.4±3.6
Antipsychotics ^a	-	-	6692.71±6254.18
Cannabis (lifetime) ^b	7.8±21.9	19.3±37.2	44.0±47.0
Other drugs (lifetime) ^b	0.90±4.7	6.2±31.4	42.4±90.8
Alcohol ^c	5.0±7.0	9.8±17.3	5.0±9.1
PANSS			
Positive symptoms	7.3±1.1	7.3±0.9	10.4±5.0
Negative symptoms	8.2±1.0	8.4±2.0	12.0±5.9
Disorganization	10.2±1.2	10.3±0.7	12.5±4.1
Excitement	8.3±1.1	8.6±1.4	9.7±2.7
Emotional distress	9.2±2.1	9.9±2.6	13.2±5.2

Means ± standard deviations are reported.

Abbreviations: PANSS, Positive and Negative Syndrome Scale

^a Lifetime exposure in haloperidol equivalents.

^b Lifetime mean number of times of substance use.

^c Weekly consumption during last 12 months.

Table 2. Number of significant voxels by fiber type for the geometrical DWI measures (case linear (CL), case planar (CP) and case spherical (CS)) in the group comparisons.

	CL		CP		CS	
	Patients	Patients	Patients	Siblings	Patients	Patients
	<	<	<	<	>	>
Type	controls	siblings	controls	controls	controls	siblings
Total						
Projection	1743	4696	2602	1215	8485	6594
Association	930	1719	34	0	3532	1836
Commissural	2042	4045	3862	2985	5594	5479
Left						
Projection	388	1963	2064	948	4072	3569
Association	374	808	34	0	1820	1155
Commissural	916	2057	1991	1871	2810	2777
Right						
Projection	1355	2733	538	267	4413	3025
Association	556	911	0	0	1712	681
Commissural	1126	1988	1871	1114	2784	2702

Results from tract-based spatial statistics. Table shows number of voxels at the $P < 0.05$ threshold.

Note: Not all significant voxels were labeled, because the atlas did not cover the entire skeleton.

Highlights

- Patients with psychotic disorder showed less fiber orientation than controls
- Patients with psychotic disorder showed less free water movement than controls
- Decreased fiber orientation may be a marker of vulnerability for psychotic disorder

ACCEPTED MANUSCRIPT